Synthesis and Characterization of Indolo[3,2-b]indole Based Copolymers for Bulk Heterojunction Polymer Solar Cell

Sung-Ho Jin[a], Hyunyoung Yoo[a], Chikyu Lee[a], Chinnusamy Saravanan[a],
Yeong-Soon Gal[b] & Jae Wook Lee[c]

[a] Department of Chemistry Education, Graduate Department of
Chemical Materials and Institute for Plastic Information and Energy
Materials, Pusan National University, Busan, Republic of Korea

[b] Polymer Chemistry Lab., Kyungil University, Hayang, Republic of
Korea

[c] Department of Chemistry, Dong-A University, Busan, Republic of
Korea
Published online: 17 Nov 2014.

PLEASE SCROLL DOWN FOR ARTICLE

Taylor & Francis
Taylor & Francis Group

Synthesis and Characterization of Indolo[3,2-b]indole Based Copolymers for Bulk Heterojunction Polymer Solar Cell

SUNG-HO JIN,[1,*] HYUNYOUNG YOO,[1] CHIKYU LEE,[1]
CHINNUSAMY SARAVANAN,[1] YEONG-SOON GAL,[2]
AND JAE WOOK LEE[3,*]

[1]Department of Chemistry Education, Graduate Department of Chemical Materials and Institute for Plastic Information and Energy Materials, Pusan National University, Busan, Republic of Korea
[2]Polymer Chemistry Lab., Kyungil University, Hayang, Republic of Korea
[3]Department of Chemistry, Dong-A University, Busan, Republic of Korea

A series of donor-acceptor low band gap polymers (DINIBT-C8, DINIBT-C10 and DINIBT-EH) containing 5,10-dihydroindolo[3,2-b]indole (DINI) as an electron donating unit and benzothiadiazole (BT) as an electron accepting unit with various kinds of alkyl chains (octyl; C8, decyl; C10 and ethyl hexyl; EH) on the donor unit have been designed, synthesized, and characterized for bulk heterojunction polymer solar cell applications. Due to the presence of long alkyl chains on the donor unit, all the polymers showing good solubility in common organic solvents. The frontier orbital energy levels of polymers were calculated using cyclic voltametry analysis. The influence of alkyl chains on the photo-physical properties of polymers were carried out. Among the three polymers, the **DINIBT-C8** *shows higher absorption coverage and good energy level matching with acceptor PC$_{71}$BM than that of the other two polymers. Thus, the bulk-heterojunction polymer solar cells (BHJ PSCs) were fabricated using* **DINIBT-C8**:*PC$_{71}$BM as an active layer with the configuration of ITO/PEDOT/* **DINIBT-C8**:*PC$_{71}$BM/LiF/Al. The* **DINIBT-C8** *shows the maximum PCE of 0.16%.*

Keywords Bulk heterojunction polymer solar cell; 5,10-dihydroindolo[3,2-b]indole (DINI); low-band gap polymers; benzothiadiazole

Introduction

The donor/acceptor low band gap polymers for bulk heterojunction (BHJ) polymer solar cells (PSCs) have been studied intensively in the recent years because of their potential utility as low-cost, large-area, flexible, light-weight roll to roll printing devices [1, 2].

*Address correspondence to Sung-Ho Jin, Department of Chemistry Education, Graduate Department of Chemical Materials, and Institute for Plastic Information and Energy Materials, Pusan National University, Busan 609-735, Korea. E-mail: shjin@pusan.ac.kr and Jae Wook Lee, Department of Chemistry, Dong-A University, Busan 604-714, Korea. E-mail: jlee@donga.ac.kr.

Color versions of one or more of the figures in the article can be found online at www.tandfonline.com/gmcl.

The BHJ, which is formed in the active layer of PSCs by the binary blending of p-type π-conjugated low band gap polymers and n-type fullerene derivatives, have offered a potential platform for dissociation of exciton into free carriers. Generally, the excitons generated in polymeric material moves towards the D/A interfaces and dissociate into free carriers with the aid of the energetic driving force originating from the differences in the electronic levels of the donor (D)/acceptor (A) materials [3, 4]. Thus, the nature of BHJ highly depended on the energy levels, miscibility, planarity of p-type donor polymers/n-type acceptor fullerene derivatives. To this end, the benchmark BHJ PSCs based on poly (3-hexylthiophene) (P3HT) and acceptor [6,6]-phenyl-C_{61}-butyric acid methyl ester (PCBM) shows the average power conversion efficiencies (PCEs) of around 4–5% under AM 1.5 conditions [5, 6]. In order to get further improvement in the efficiency of PSCs, many kinds of donor/acceptor low band gap copolymers have been designed, synthesized and utilized for PSCs [7]. Particularly, the carbazole based copolymers has become the next benchmark structure among the most efficient, stable and low-cost material for BHJ PSCs [8].

The size and density of solubilizing alkyl chains on the polymer backbone plays an important role in the determination of the morphology of the active layer, which also one of the detrimental factor on the PCE of PSCs [9]. In order to facilitate the formation of nanoscale phase separation in the active layer of PSCs, the systematic analysis of the position and nature of alkyl chains of the particular polymer is very important. Very recently, Owczarczyk et al. have estabilzied donor−acceptor copolymers containing 5,10-dihydroindolo[3,2-b]indole (DINI) as electron donor unit and diketopyrrolopyrrole and thienopyrroledione as the electron accepting units, which are the derivative of carbazole, for BHJ PSCs [10]. Here, they explored the size and shape of the pendant alkyl substituents attached to the DINI unit on the optical and electronic properties of the copolymers. In this work, we have synthesized a series of copolymers containing the DINI as an electron donor unit with various kinds alkyl chains on the nitrogen atoms and the benzothiadiazole (BT) as electron accepting unit for BHJ PSC applications as shown in Scheme 1.

Experimental

Materials

All the chemicals and reagents purchased from Sigma-Aldirich were used without any further purification. The 2,1,3-benzothiadiazole-4,7-bis(boronic acid pinacol ester) and tetra-n-buytylammonium tetrafluroborate (TBABF$_4$) were also purchased from Sigma-Aldrich and used as received. The 5,10-dihydroindolo[3,2-b]indole (**3**) was prepared according to the reported procedures [10].

Synthesis of 5,10-dioctyl-5,10-dihydroindolo[3,2-b]-indole (4)

To a stirred of a solution of 1.24 g (6.02 mmol) of compound 3 in 55 mL of THF at room temperature under nitrogen was added 576 mg (18.06 mmol) of NaH in 40 mL of THF. After 10 min at room temperature, 4.65 g (24.08 mmol) of n-bromooctane was added to the reaction mixture. The resultant mixture was refluxed for overnight, treated with 60 mL of water, extracted using 3×30 mL of methylene chloride, washed with water and brine and dried over anhydrous MgSO$_4$. The solvents was removed under reduced pressure and purified by flash silica gel column chromatography (hexane) to give 1.17 g (45%) of compound 4 as a white solid.
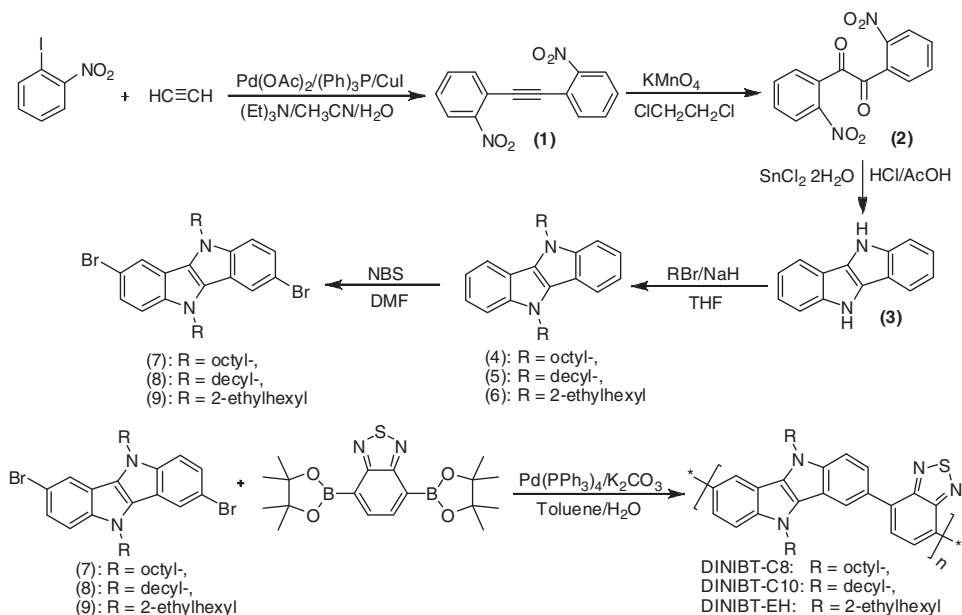
Scheme 1. Synthesis of **DINIBT-C8**, **DINIBT-C10** and **DINIBT-EH**.

^{1}H-NMR (CDCl$_3$, ppm): 0.84 (t, 6H), 1.41 (m, 20H), 1.92 (m, 4H), 4.61 (t, 4H), 7.15 (t, 2H), 7.29 (t, 2H), 7.60 (d, 2H),7.92 (d, 2H); ^{13}C-NMR (CDCl$_3$, ppm): 14.27, 22.92, 27.25, 29.30, 29.73, 30.31, 32.01, 45.61, 109.86, 114.65, 116.78, 118.07, 121.62, 126.01, 141.73.

Synthesis of 5,10-didecyl-5,10-dihydroindolo[3,2-b]-indole (5)

The compound **5** was synthesized as white colored solid with a quantitative yield using the similar procedure for compound **4**.

^{1}H-NMR (CDCl$_3$, ppm): 0.84 (t, 6H), 1.41 (m, 28H), 1.92 (m, 4H), 4.61 (t, 4H), 7.15 (t, 2H), 7.29 (t, 2H), 7.60 (d, 2H),7.92 (d, 2H); ^{13}C-NMR (CDCl$_3$, ppm): 14.39, 22.94, 27.43, 29.54, 29.70, 29.76, 29.81, 30.57, 32.13, 45.56, 109.96, 114.76, 116.88, 118.18, 121.71, 126.08, 141.74.

Synthesis of 5,10-di-2-ethylhexyl-5,10-dihydroindolo[3,2-b]-indole (6)

The compound **6** was also prepared as white colored solid with a quantitative yield by adopting the similar procedure for compound **4**.

^{1}H-NMR (CDCl$_3$, ppm): 0.84 (t, 12H), 1.41 (m,14H), 1.92 (m, 4H), 4.61 (t, 4H), 7.15 (t, 2H), 7.29 (t, 2H), 7.60 (d, 2H),7.92 (d, 2H); ^{13}C-NMR (CDCl$_3$, ppm): 11.04, 14.25, 23.24, 24.50, 28.94, 31.09, 39.48, 47.33, 109.75, 114.64, 116.76, 118.05, 121.60, 125.97, 141.62.

Synthesis of 2,7-Dibromo-5,10-dioctyl-5,10-dihydroindolo[3,2-b]-indole (7)

To a stirred solution of 1.17 g (2.72 mmol) of compound **4** in dimethylformamide (100 mL) at 0°C under nitrogen was slowly added 0.97 g (5.44 mmol) of N-bromosuccinimide in

dimethylformamide (50 mL). After stirring for 3 hrs at room temperature, the reaction mixture was poured into water (100 mL) and the resulting white precipitate was filtered and dried. The crude product was purified by flash silica gel chromatography (hexane) to give 510 mg (32%) of compound 7 as a colorless solid. The compounds **8** and **9** were also prepared by applying this procedure.

^{1}H-NMR (CDCl$_3$, ppm): 0.85 (t, 6H), 1.23 (m, 12H), 1.32 (m, 4H), 1.38 (m, 4H), 1.93 (m, 4H), 4.43 (t, 4H), 7.27 (dd, 2H), 7.63 (s, 2H), 7.69 (d, 2H); ^{13}C-NMR (CDCl$_3$, ppm): 14.26, 22.93, 27.25, 29.30, 29.74, 30.32, 32.02, 45.74, 112.96, 113.37, 115.68, 118.82, 121.64, 126.02, 141.37.

Synthesis of 2,7-Dibromo-5,10-didecyl-5,10-dihydroindolo[3,2-b]-indole (8)

^{1}H-NMR (CDCl$_3$, ppm): 0.84 (t, 6H,), 1.30 (m, 28H), 1.90 (m, 4H), 4.61 (t, 4H), 7.25 (dd, 2H), 7.58 (s, 2H), 7.64 (d, 2H); ^{13}C-NMR (CDCl$_3$, ppm): 14.38, 22.93, 27.43, 29.52, 29.71, 29.77, 29.82, 30.55, 32.14, 45.55, 112.97, 113.38, 115.66, 118.83, 121.68, 126.01, 141.35.

Synthesis of 2,7-Dibromo-5,10-di-2-ethylhexyl-5,10-dihydroindolo[3,2-b]-indole (9)

^{1}H-NMR (CDCl$_3$, ppm): 0.84 (t, 12H), 1.30 (m, 14H), 1.90 (m, 4H), 4.61 (t, 4H), 7.25 (dd, 2H), 7.58 (s, 2H), 7.64 (d, 2H); ^{13}C-NMR (CDCl$_3$, ppm): 11.04, 14.25, 23.24, 24.50, 28.94, 31.09, 39.48, 47.33, 112.93, 113.34, 115.63, 118.80, 121.65, 126.03, 141.35.

Synthesis of DINIBT-C8

Under Nitrogen atmosphere, the compound **7** (176.5 mg, 0.3 mmol), 2,1,3-benzothiadiazole-4,7-bis(boronic acid pinacol ester) (116.4 mg, 0.3 mmol), tetrakis(triph enylphosphine)palladium(0) (17.3 mg, 0.015 mmol) were added into 25 ml round flask. Freshly distilled toluene (1 mL) was added and the mixture was stirred at 120°C for 5 minutes. Then, 2 M K$_2$CO$_3$ (1 mL) was injected slowly into the reaction and stirred for 2 days. To complete the end-capping reaction, bromobenzene and phenylboronic acid was added into the reaction mixture with an appropriate time gap. After completion of reaction, the mixture allowed to cool room temperature and poured into methanol. A solid was obtained by filtration. The polymer was further purified by stirring it in methanol and acetone for 24 hours and passed through celite to remove oligomers and catalyst residues. After precipitating the resulting product in methanol, it was dried under reduced pressure. The polymer **DINIBT-C8** was obtained as dark brown colored solid.

^{1}H-NMR (CDCl$_3$, ppm): 0.84 (s, 6H,), 1.30 (m, 20H), 1.91 (br, 4H), 4.63 (br, 4H), 7.27–8.23 (br, 8H); ^{13}C-NMR (CDCl$_3$, ppm): 14.37, 22.96, 27.23, 29.32, 29.62, 30.51, 32.12, 45.53, 111.15, 114.31, 117.56, 119.43, 127.21, 128.11, 131.32, 132.43, 141.10, 154.41; Anal Calcd for C$_{36}$H$_{42}$N$_4$S : C, 76.55; H, 7.85; N, 9.92. Found: C, 76.05; H, 7.82; N, 9.55.

Synthesis of DINIBT-C10

The polymer **DINIBT-C10** was also prepared by applying procedure similar for **DINIBT-C8**.

^{1}H-NMR (CDCl$_3$, ppm): 0.84 (s, 6H,), 1.30 (m, 28H), 1.90 (br, 4H), 4.61 (br, 4H), 7.27–8.23 (br, 8H); ^{13}C-NMR (CDCl$_3$, ppm): 14.38, 22.93, 27.43, 29.52, 29.71, 29.77, 29.82, 30.55, 32.14, 45.55, 111.17, 114.35, 117.66, 119.63, 127.36, 128.31, 131.24, 132.40,

141.15, 154.42. Anal Calcd for $C_{36}H_{42}N_4S$: C, 77.37; H, 8.44; N, 9.02. Found: C, 76.92; H, 8.26; N, 8.92.

Synthesis of DINIBT-EH

The polymer **DINIBT-EH** was also synthesized by adopting similar procedure for **DINIBT-C8**.

   ^{1}H-NMR (CDCl$_3$, ppm): 0.84 (s, 12H,), 1.30 (m, 14H), 1.91 (br, 4H), 4.63 (br, 4H), 7.27–8.23 (br, 8H); ^{13}C-NMR (CDCl$_3$, ppm): 11.02, 14.15, 23.18, 24.45, 28.89, 31.12, 39.47, 47.23, 111.16, 114.33, 117.63, 119.61, 127.34, 128.27, 131.18, 132.24, 141.11, 154.40. Anal Calcd for $C_{36}H_{42}N_4S$: C, 76.55; H, 7.85; N, 9.92. Found: C, 76.25; H, 7.75; N, 9.03.

Fabrication of Organic Photovoltaic Cells

The glass substrates were coated with a transparent ITO electrode (110 nm thick, 10~15 Ω / sq sheet resistance), which was ultrasonically cleaned with detergent, distilled water, acetone, and isopropyl alcohol (IPA). Then, the layer of 40 nm thick PEDOT:PSS (baytron P) was spun-coated onto the pre-cleaned and UV-ozone treated ITO substrates and the film baked in air at 150°C for 30 minutes. The solution of active layer, which was prepared by dissolving appropriate ratios of PIIBT-C8/PCBM in chloroform/*o*-dichlorobenzene (1:1, v/v) co-solvent system, was filtered with 0.45 μm PTFE (hydrophobic) syringe filter and spin coated on the top of the PEDOT:PSS with the layer thickness of 80~90 nm, dried at room temperature for 30–40 minute. The Lithium fluoride (LiF) (0.5 nm) and Aluminum (Al) cathode (120 nm) were deposited on the top of the active layer under vacuum less than 5.0×10^{-6} torr, which yields a 9 mm^2 of active area per each pixel. The film thickness was measured with a α-Step IQ surface profiler (KLA Tencor, San Jose, CA). The fabricated BHJ PSCs performance was measured by using photocurrent density-voltage (J-V) characteristics under light illumination. To characterize the OPV cells, measurement was carried out using a Solar Simulator (Orel 300 W simulator, models 81150) under a simulated solar light with ARC Lamp power supply (AM 1.5G, 100 mW/cm^2) and a standard source measure unit (Keithley 236). All processes and measurements mentioned above were carried out in the open air at room temperature.

Results and Discussion

Scheme 1 shows the synthetic routes for the monomers and polymers. In the first step, iodo-2-nitrobenzene was treated with acetylene gas in the presence of palladium diacetate, triphenylphosphine, and cuprous iodide in acetonitrile and water to generate the compound **1**, which was oxidized in the presence of KMnO$_4$ in water and methylene chloride to gives the compound **2**. It was reduced using stannous chloride dihydrate in the mixture of acetic acid and hydrochloric acid to give compound **3** [10]. The compound **3** was alkylated using NaH in THF with n-bromooctane, n-bromodecane and 2-ethylhexylbromide afford compound **4**, **5** and **6** with quantitative yields, respectively. The compounds **4**, **5** and **6** were brominated using NBS in DMF yields monomers **7**, **8**, and **9** with good yield, respectively. These monomers, **7**, **8** and **9**, were polymerized with another monomer, 2,1,3-Benzothiadiazole-4,7-bis(boronic acid pinacol ester), by Suzuki polymerization to get the corresponding polymers **DINIBT-C8**, **DINIBT-C10** and **DINIBT-EH**, respectively. After polymerization, all the polymers were precipitated into methanol and purified by Soxhlet

Table 1. Physical properties of DINIBT-C8, DINIBT-C10 and DINIBT-EH

Polymer	Mn[a]	Mw[a]	PDI[a]	T_d[b] (°C)	$\lambda_{abs\,max}$[c] (nm)	λ_{em}[c] (nm)	HOMO[d] (eV)	LUMO[e] (eV)	Eg[f] (eV)
DINIBT-C8	7530	14100	1.88	347	385, 552	649	−5.01	−3.13	1.88
DINIBT-C10	9400	14600	1.56	333	370, 533	671	−5.03	−3.11	1.92
DINIBT-EH	9020	17200	1.91	401	371, 501	660	−5.02	−3.10	1.92

[a]Mn, Mw and PDI of the polymers were determined by GPC using polystyrene standards; [b]T_d was determined from TGA thermograms; [c]measured in the thin film onto the quartz substrate; [d]measured in acetonirtile with 0.1M TBABF$_4$ (film onto a counter electrode) HOMO (eV) = −4.8 - (E_{onset} - $E_{1/2}$(Ferrocene)); [d]estimated from HOMO levels and the optical band gaps: LUMO = HOMO + Eg; [f]determined from UV–visible absorption.

extraction in acetone and hexane to remove catalytic impurities and low molecular weight oligomers. Under these processes, the high pure and narrow dispersed polymers were obtained. Details of molecular weights and polydispersity index (PDI) values of all the polymers are shown in Table 1. All the polymers have good solubility in common solvents such as chloroform, toluene, tetrahydrofuran, etc. Molecular structures of the monomers and polymers were confirmed by ^{1}H-NMR and ^{13}C-NMR spectroscopy.

The thermal properties of all the polymers were investigated by TGA and DSC thermal analysis and the corresponding TGA and DSC thermograms of all the polymers are shown in Fig. 1. From the TGA thermogram, the onset decomposition temperature of DINIBT-C8, DINIBT-C10 and DINIBT-EH were found to be 347°C, 333°C and 401°C, respectively. Among the three polymers, the DINIBT-C10 has less thermal stability than the other two polymers due to the presence of longer alkyl chain. Particularly, DINIBT-EH shows higher
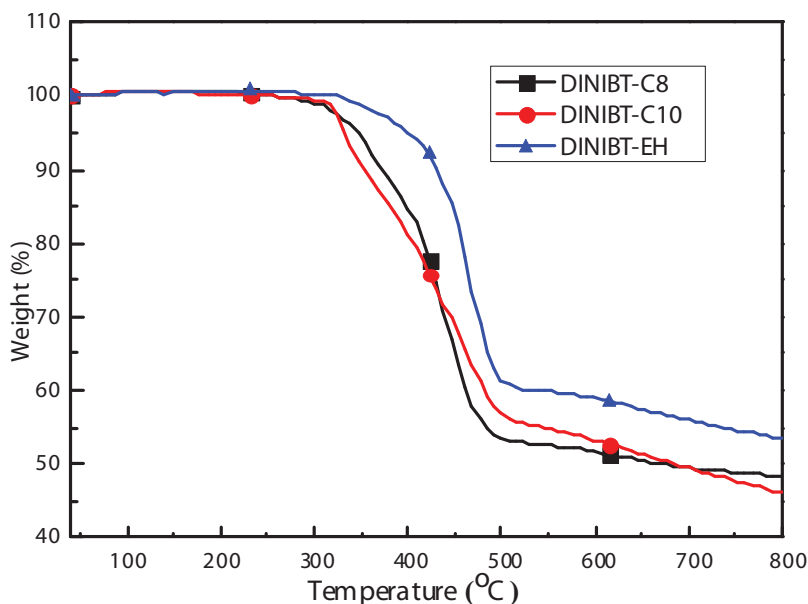
Figure 1. TGA thermograms of **DINIBT-C8**, **DINIBT-C10** and **DINIBT-EH.**
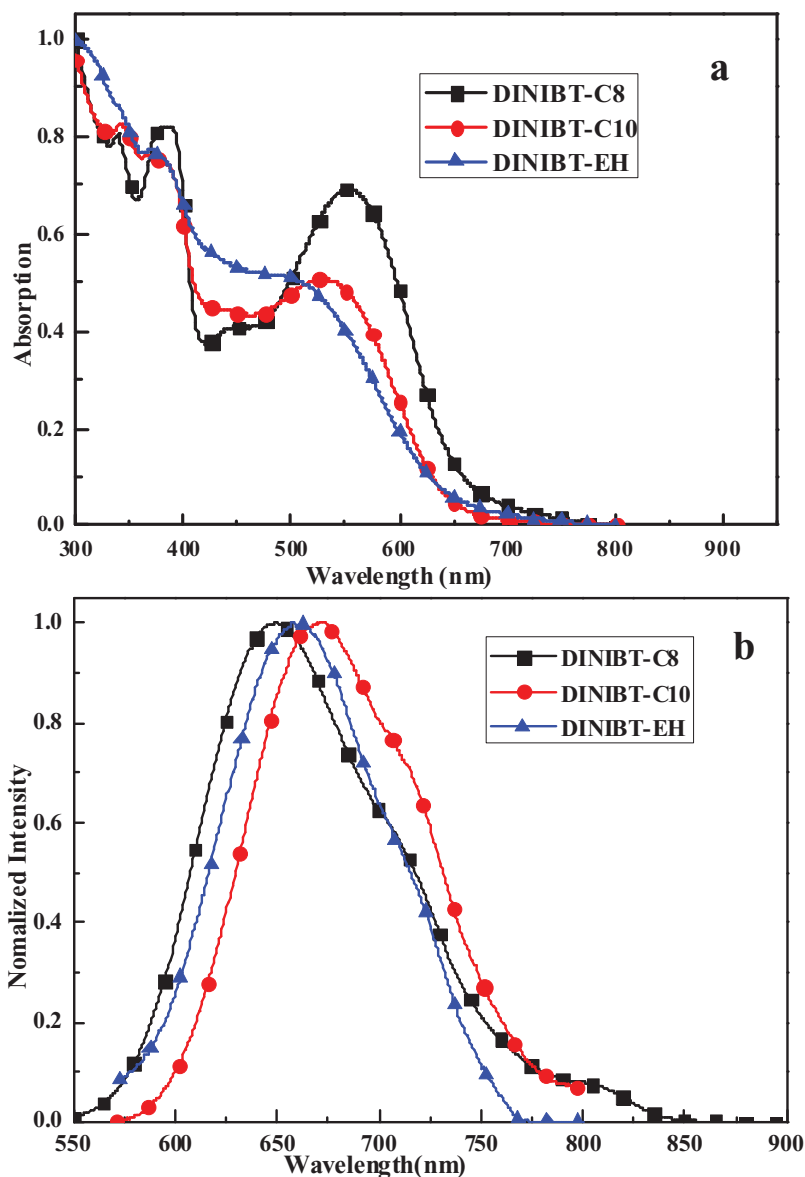
Figure 2. a) UV-visible absorption and b) fluorescence spectra of **DINIBT-C8**, **DINIBT-C10** and **DINIBT-EH** in thin film.

thermal stability due to the presence of branched alkyl chain that is suitable to form a stable solid state. The glass transition temperature of all the polymers is invisible.

In order to understand the absorption coverage of all the polymers, the UV-visible absorption spectra of thin films of all the polymers were measured and corresponding absorption spectra are shown in Fig. 2a. The thin films were prepared by spun coating of corresponding chloroform solution onto a quartz slide. All the polymers show two absorption bands; the bands in the high energy regions corresponding to the π-π^* transition of aromatic moieties and the bands at lower energy regions are corresponding to the intra

molecular charge transfer (ICT) between DINI and BT entities. The DINIBT-C8, DINIBT-C10 and DINIBT-EH show the absorption maxima at 385 nm & 552 nm, 370 nm & 533 nm and 371 nm & 501 nm, respectively. Among the three polymers, the DINIBT-C8 shows broad and red shifted ICT band than the DINIBT-C10 and DINIBT-EH. It suggests that the orientation of octyl chains in the solid state is more favorable for the efficient ICT interactions between DINI and BT units. Particularly, the higher energy bands do not show any significant changes with respect to the nature of aliphatic chains. The emission spectra of thin films of all these polymers are shown in Fig. 2b. When increasing the length of aliphatic chain from DINIBT-C8 to DINIBT-C10, the emission maxima was shifted from 649 nm to 671 nm and the DINIBT-EH shows an emission maximum at 660 nm.

To investigate the information about the charge injection and devices performance, it is very important to calculate the frontier orbital (highest occupied molecular orbital (HOMO) and lowest unoccupied molecular orbital (LUMO)) energy levels of all the polymers. The HOMO of the all the polymers were measured from the cyclic voltametry (CV) and the optical band gap from optical absorption spectra. The CV experiments of all the polymers were carried out with $TBABF_4$ (0.1 M in acetonitrile) as electrolyte at a scan rate of 50−100 mV/s. Here, each polymer film as working electrode, platinum wire as the counter electrode and Ag/AgCl as reference electrode was used to measure the cyclic voltammograms. The potentials were calibrated with ferrocene/ferrocenium redox couple (Fc/Fc^+). The cyclic voltammograms of all the polymers are shown in Fig. 3 and the electrochemical values are extracted in Table 1. By assuming the energy level of Fc/Fc+ to be −4.8 eV below the vaccum level, the HOMO level of polymer was determined by $E_{HOMO} = -4.8 - (E_{ox,onset} - E_{1/2}$ (ferrocence)) eV. The LUMO levels were measured by $E_{LUMO} = E_{HOMO} + Eg$ eV. Accordingly, the HOMO/LUMO energy levels of **DINIBT-C8**, **DINIBT-C10** and **DINIBT-EH** were found to be −5.01/−3.13 eV, −5.03/−3.11 eV and
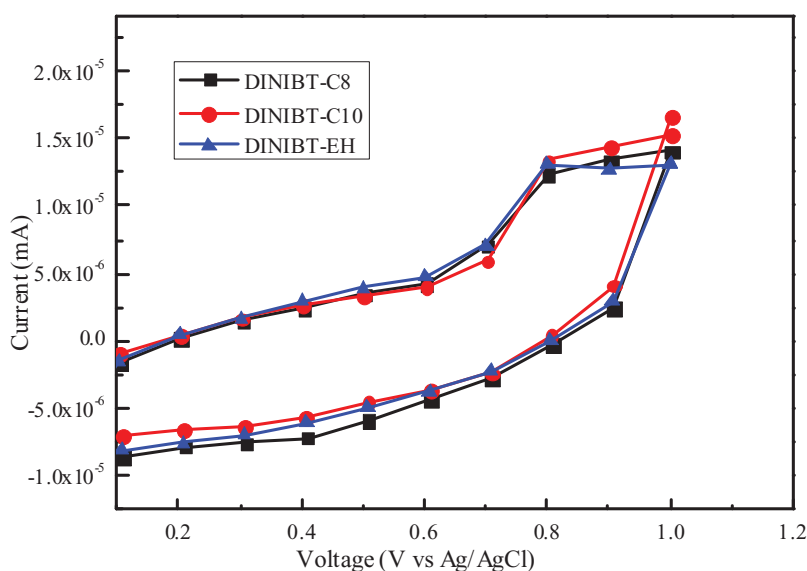

Figure 3. Cyclic voltammograms of **DINIBT-C8**, **DINIBT-C10** and **DINIBT-EH** thin films in 0.1 M $TBABF_4$ solution in acetonitrile at a scan rate of 100 mV/s.
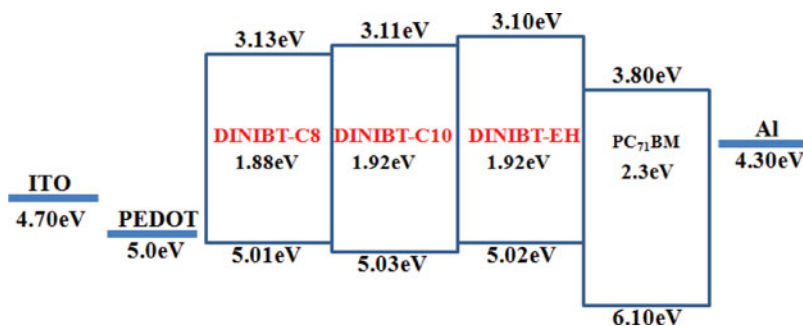
Figure 4. Energy level diagram of **DINIBT-C8, DINIBT-C10,− DINIBT-EH** and PC$_{71}$BM.

−5.02/−3.10 eV and the corresponding band gaps are 1.88 eV, 1.92 eV and 1.92 eV, respectively. These energy levels polymers are well matched with the energy levels of PC$_{71}$BM acceptor, which is more favorable for the dissociation of exciton at the interface between the donor and acceptor. The corresponding energy level diagram was shown in Fig. 4.

Due to the favorable optical properties and well matched energy levels with PC$_{71}$BM, The BHJ PSCs were fabricated using the polymer **DINIBT-C8** as an electron donor and PC$_{71}$BM as an electron acceptor. The devices were fabricated with the configuration of ITO (110 nm)/ PEDOT:PSS (40 nm)/DINIBT-C8:PCBM (80 nm)/LiF (0.5 nm)/Al (120 nm) and the corresponding current density- voltage curves (J-V) under the illumination of AM 1.5G (100 mW/cm^2) are shown in Fig. 5. The device parameters are extracted in Table 2. As shown in Table 2, upon increasing the ratio of PC$_{71}$BM content in the active layer of the devices, the J$_{sc}$ is increased from 0.58 mA/cm^2 to 0.76 mA/cm^2 results to increase the
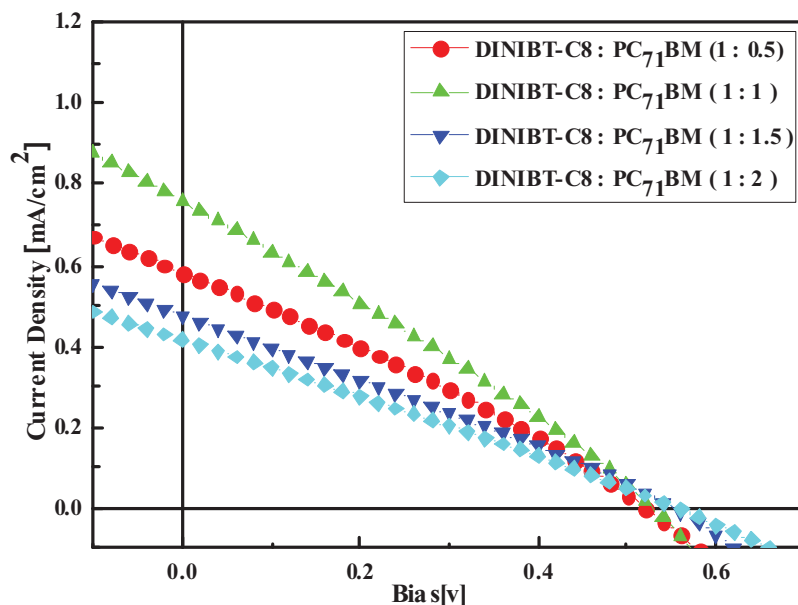

Figure 5. The current density-voltage (J-V) characteristics of devices based on **DINIBT-C8**:PC$_{71}$BM with different ratios of PC$_{71}$BM.

Table 2. Photovoltaic performance of devices based on DINIBT-C8:PC$_{71}$BM with various ratios of PC$_{71}$BM under AM 1.5G illumination (100 mW/cm^2)

Active layer	V_{oc}[a] (V)	J_{sc}[b] (mA/cm^2)	FF[c] (%)	PCE[d] (%)
DINIBT-C8:PC$_{71}$BM (1:0.5)	0.52	0.58	29.05	0.088
DINIBT-C8:PC$_{71}$BM (1:1)	0.53	0.76	27.95	0.112
DINIBT-C8:PC$_{71}$BM (1:1.5)	0.55	0.48	26.78	0.070
DINIBT-C8:PC$_{71}$BM (1:2)	0.55	0.41	26.49	0.061

[a]J_{sc}: short-circuit current density; [b]V_{oc}: open-circuit voltage; [c]FF: fill factor; [d]PCE: power conversion efficiency.

Table 3. Photovoltaic performance of devices based on DINIBT-C8:PC$_{71}$BM with various annealing temperatures under AM 1.5G illumination (100 mW/cm^2)

Active layer	Annealing temp. (°C)	V_{oc} (V)	J_{sc} (mA/cm^2)	FF (%)	PCE (%)
DINIBT-C8:PC$_{71}$BM	—	0.55	0.70	27.92	0.11
DINIBT-C8:PC$_{71}$BM	80	0.56	0.95	29.72	0.15
DINIBT-C8:PC$_{71}$BM	100	0.55	0.94	28.86	0.14
DINIBT-C8:PC$_{71}$BM	120	0.54	1.01	29.96	0.16

[a]J_{sc}: short-circuit current density; [b]V_{oc}: open-circuit voltage; [c]FF: fill factor; [d]PCE: power conversion efficiency.
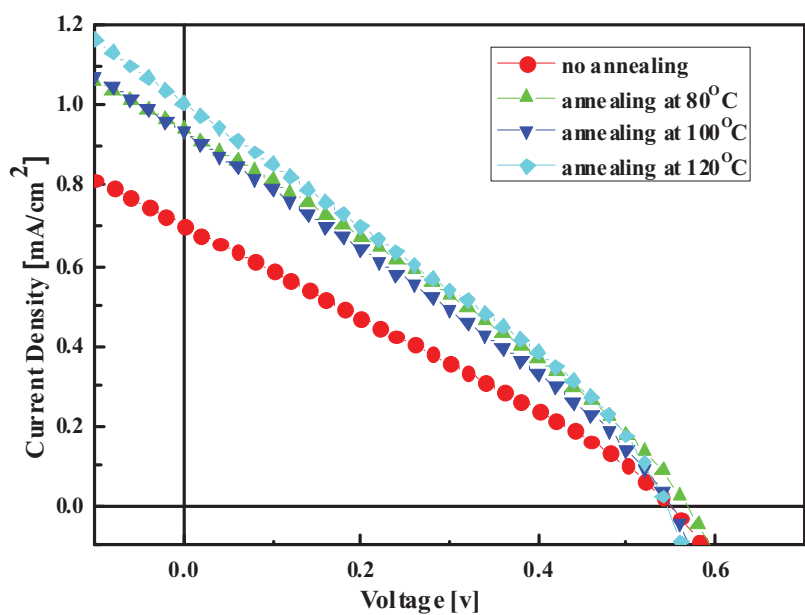

Figure 6. The current density-voltage (J-V) curves of **DINIBT-C8**:PC$_{71}$BM based devices with various annealing temperatures for 30 min.

PCE from 0.09% to 0.11%. Further increasing the ratio of PCBM, the efficiency going to decrease. With all the ratios of $PC_{71}BM$, there are no significant changes in the V_{oc}, due to the fact that V_{oc} is depending on the HOMO of the donor polymer and LUMO of the acceptor. Thus, the optimized ratio of the **DINIBT-C8**:$PC_{71}BM$ is 1:1. In order to increase the efficiency of the devices, the annealing temperature of the devices were optimized. Upon increasing the annealing temperature from 80°C to 120°C, the efficiency is increased from 0.11% to 0.16% and corresponding J-V curves and device characteristics are shown in Fig. 6 and Table 3, respectively.

Conclusions

In summary, we have designed and synthesized a series of low band gap copolymers, containing DINI donor unit and BT acceptor unit for BHJ PSCs applications. All the polymers showing better solubility in common organic solvents and exhibit narrow band gap less than 2.0 eV. The absorption spectra of all the polymers covers from 300 to 700 nm region. Among the absorption spectra of thin films of all polymers, the **DINIBT-C8** shows well defined ICT absorption band, which confirms that the octyl chain on the nitrogen atom of DINI offers a more favorable environment for ICT interactions between the donor and acceptor units. Thus, we fabricated BHJ PSCs using the **DINIBT-C8**:$PC_{71}BM$ blend as the active layer and observed the optimized PCE of 0.11%. Upon annealing the optimized devices with various temperatures, it shows the maximum PCE of 0.16% with annealing temperature at 120°C for 30 mins. In order to further improvement in the efficiency of these polymers, the another derivatives of these moieties are currently underway.

Acknowledgments

References

[1] Ling, Y., Wu, Y., Feng, D., Tsai, S. T., Son, H. J., Li, G., & Yu, L. (2009). *J. Am. Chem. Soc.*, *131*, 56.

[2] Hoppe, H., & Sariciftci, N. S. (2004). *J. Mater. Res.*, *19*, 1924.

[3] Sariciftci, N. S., Smilowitz, L., Heeger, A. J., & Wudl, F. (1992). *Science*, *258*, 1474.

[4] Halls, J. J. M., Pichler, K., Friend, R. H., Moratti, S. C., & Holmes, A. B. (1996). *Appl. Phys. Lett.*, *68*, 3120.

[5] Reyes-Reyes, M., Kim, K., & Carroll, D. L. (2005). *Appl. Phys. Lett.*, *87*, 083506.

[6] Ma, W., Yang, C., Gong, X., Lee, K., & Heeger, A. J. (2005). *Adv. Funct. Mater.*, *15*, 1617.

[7] Cheng, Y.-J., Yang, S.-H., & Hsu, C.-S. (2009). *Chem. Rev.*, *109*, 5868.

[8] Beaupre, S., & Leclerc, M. (2013). *J. Mater. Chem. A*. DOI: 10.1039/C3TA12420G.

[9] Mayer, A. C.; *et al.* (2009). *Adv. Funct. Mater.*, *19*, 1173.

[10] Owczarczyk, Z. R., Braunecker, W. A., Garcia, A., Larsen, R., Nardes, A. M., Kopidakis, N., Ginley, D. S., & Olson, D. C. (2013). *Macromolecules*, *46*, 1350.